On-Target Contrast Diagnostic via Specular Reflectivity Measurement

A. S. Pirozhkov,[a] I. W. Choi,[b] J. H. Sung,[b] S. K. Lee,[b] T. J. Yu,[b] T. M. Jeong,[b] I J. Kim,[b] N. Hafz,[b] C. M. Kim,[b] K. H. Pae,[b] Y.-C. Noh,[b] D.-K. Ko,[b] J. Lee,[b] A. Robinson,[c] P. Foster,[c] S. Hawkes,[c] M. Streeter,[c] C. Spindloe,[c] P. McKenna,[d] D. C. Carroll,[d] C.-G. Wahlström,[e] M. Zepf,[f] B. Dromey,[f] K. Markey,[f] S. Kar,[f] Y. T. Li,[g] M. H. Xu,[g] H. Nagatomo,[h] M. Mori,[a] A. Yogo,[a] H. Kiriyama,[a] K. Ogura,[a] A. Sagisaka,[a] S. Orimo,[a] M. Nishiuchi,[a] H. Sugiyama,[a] T. Zh. Esirkepov,[a] H. Okada,[a] S. Kondo,[a] S. Kanazawa,[a] Y. Nakai,[a] A. Akutsu,[a] T. Motomura,[a] M. Tanoue,[a] T. Shimomura,[a] M. Ikegami,[a] I. Daito,[a] M. Kando,[a] T. Kameshima,[a] P. Bolton,[a] S. V. Bulanov,[a] H. Daido,[a] and D. Neely[c]

[a] *Advanced Photon Research Center and Photo-Medical Research Center, Japan Atomic Energy Agency, 8-1-7 Umemidai, Kizugawa, Kyoto, 619-0215, Japan.*
[b] *Center for Femto-Atto Science and Technology, Advanced Photonics Research Institute, GIST, 1 Oryong-dong, Buk-gu, Gwangju 500-712, Korea*
[c] *Central Laser Facility, STFC, Rutherford Appleton Laboratory, Didcot OX11 0QX, UK*
[d] *SUPA, Department of Physics, University of Strathclyde, Glasgow G4 0NG, UK*
[e] *Department of Physics, Lund University, P.O. Box 118, S-22100 Lund, Sweden*
[f] *Department of Physics and Astronomy, Queens University Belfast, BT7 1NN, Northern Ireland, UK*
[g] *Laboratory of Optical Physics, Institute of Physics, Beijing 100190, China*
[h] *Institute of Laser Engineering, Osaka University, 2-6 Yamada-oka, Suita, Osaka 565-0871, Japan*

Abstract. High-power laser contrast is challenging to measure, especially in the real target irradiation conditions. We present a convenient and relatively simple contrast diagnostic technique based on the measurement of target specular reflectivity at full laser power. The reflectivity remains high even at intensities above 10^{19} W/cm^2 in the case of a high-contrast prepulse-free laser. On the contrary, the specular reflectivity drops in the case of lower contrast, due to the beam break-up and increased absorption caused by the preformed plasma. The technique was demonstrated using three different laser systems with several contrast conditions: Astra (CLF, RAL), TiS laser at APRI, GIST, and J-KAREN (APRC, JAEA).

Keywords: Relativistic laser plasma; High-power laser contrast; Contrast diagnostics.
PACS: 5240Nk; 5260+h

INTRODUCTION

Modern high-power laser systems can routinely achieve ultra-relativistic intensities much higher than 10^{18} W/cm^2 [1]. A target irradiated by a pulse with such intensity, however, can be destroyed or significantly altered by a light preceding the main pulse,

CP1153, *Laser-Driven Relativistic Plasmas Applied to Science, Industry and Medicine - The 2nd International Symposium*
edited by P. R. Bolton, S. V. Bulanov, and H. Daido

if the contrast is not sufficient. This preceding light includes the Amplified Spontaneous Emission (ASE) or fluorescence, Picosecond Pedestal (PP), and possible prepulses (pre). The contrast C is the ratio between the main pulse power and the power of corresponding kind of the preceding light. The typical values are $C_{ASE} \sim 10^6 - 10^{10}$, $C_{PP} \sim 10^3 - 10^5$, and $C_{pre} \sim 10^2$ to 10^6. The typical durations are $\tau_{ASE} \sim$ few ns, $\tau_{PP} \sim$ few to few tens ps, and τ_{pre} is similar or somewhat longer than the main pulse duration. It is easy to see that for an ultra-intense laser pulse the ASE, pedestal, or prepulses are able to produce plasma themselves; this plasma is called preplasma. Preplasma is in many cases very undesirable. In fact, the contrast has become a major issue in many experiments involving irradiation of solid and even gas and other lower-density targets. However, the accurate determination of contrast is still a challenge, taking into account the set of requirements: high dynamic range (10^{10} and even higher), long time measurement interval (~ few ns), high temporal resolution and small sampling interval (ideally smaller than the main pulse duration), and desirability for full-power, on-target diagnostic. The power contrast is usually measured with a high-dynamic range 3rd-order cross-correlator [2], which requires many thousands of shots. Further, cross-correlators tend to produce artificial prepulses which are difficult to distinguish from the real ones because their delays and contrasts are similar [3]. In addition, the focal spot of the ASE and prepulses may differ from that of the main pulse, so that the power and intensity contrasts are not same.

Another approach to the contrast diagnostic is measurement of preplasma parameters. The scale length of preplasma with relatively large dimension (typically > 10 μm) can be measured using imaging and interferometry [4]. Plasma XUV imaging and time-resolved emission measurement can also be used to monitor [5] the ASE. In this paper we demonstrate a complementary technique [6] which is simple, convenient and is able to determine whether the on-target contrast is sufficient or not, and in the latter case to estimate the necessary contrast improvement.

EXPERIMENTAL SETUP

The technique was demonstrated using three laser systems and different contrast conditions (Table 1). We measured the dependence of the specular reflectivity R of flat targets, irradiated with full laser power, on the target position T; the intensities of the main pulse and ASE/prepulses were thus varied by several orders of magnitude. The target position T is measured along the beam direction, with $T = 0$ corresponding to best focus. We used p-polarized pulses at 35° and 45° incidence angle, which is the typical experimental arrangement for ion acceleration and harmonic generation experiments (Fig. 1).

Experiment A was performed with Astra Ti:Sapphire laser [7] using both normal contrast and high contrast modes. The latter was achieved with the help of a Plasma Mirror [8-10] (PM). The plasma mirror reflectivity was 0.6 and the contrast improvement was ~ 10^2. Without the plasma mirror (normal contrast case), the targets were 2 μm Al plates. With the plasma mirror (high contrast case), the Al target thickness was reduced down to 50 nm.

Experiment B was performed with Ti:Sapphire laser system at Advanced Photonics Research Institute (APRI), Gwangju Institute of Science and Technology

(GIST) [11]. The targets were 7.5 and 12.5 μm polyimide tapes. Using the transmission through a polyimide target in the irradiation regimes similar to the plasma mirror, we measured the ASE energy which was ~3% of the main pulse. This agrees well with the estimations based on the ASE contrast and duration; the details of the technique will be described elsewhere.

Experiment C was performed with J-KAREN hybrid OPCPA/Ti:Sapphire laser system [12], consisting of a high-energy CPA oscillator, saturable absorber improving the system contrast, stretcher, three-stage OPCPA and two 4-pass Ti:Sapphire amplifiers. The final amplifier was cryogenically cooled to avoid thermal effects, which enabled 10 Hz operation. The target was 7.5 μm polyimide tape.

TABLE 1. On-target laser parameters. E_0, τ_0, λ_0 are the laser pulse energy, duration, and wavelength; $f/\#$ is the Off-Axis Parabola (OAP) f-number; r_0 is the focal spot radius [Half Width at Half Maximum (HWHM)]; I_0 is the peak intensity (average over FWHM) at the incidence angle θ; C_{ASE}, τ_{ASE}, and E_{ASE}/E_0 are the ASE contrast, duration, and energy fraction.

Experiment	A	A with PM	B	C
E_0, J	0.7	0.4	0.8/1.6	0.5
τ_0, fs	50	50	35	35
λ_0, nm	800	800	800	820
$f/\#$	3	3	3.4	3
r_0, μm	2.5	2.5	2.0	1.7
I_0, W/cm^2	3×10^{19}	2×10^{19}	4×10^{19}	5×10^{19}
θ, °	35	35	45	45
C_{ASE}	10^7	10^9	10^6	5×10^8
τ_{ASE}, ns	1	1	0.9	3
E_{ASE}/E_0	2×10^{-3}	2×10^{-5}	3×10^{-2}	2×10^{-4}
Target	Al 2 μm	Al 50 nm	Polyimide 7.5 and 12.5 μm	Polyimide 7.5 μm

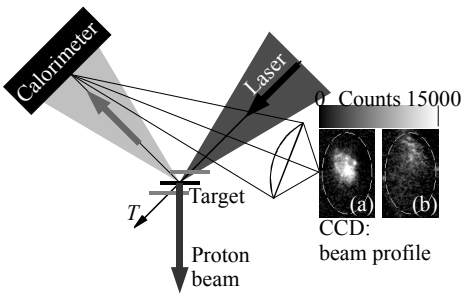

FIGURE 1. Experimental setup. Multi-TW p-polarized laser irradiates a few-μm or nm-thick target at oblique incidence (35° in the experiment A and 45° in the experiments B and C). The spot size is varied by moving the target along the laser beam. The calibrated in-vacuum calorimeter is used to measure the target specular reflectivity [Fig. 2 (a), (b)]. The lens images the calorimeter surface onto the CCD to measure the reflected beam profile; two examples from the experiment B are shown in the inset: (a) corresponds to the target position with the relatively small preplasma (T = - 1.41 mm), while (b) corresponds to the target position closer to the focus (T = - 0.71 mm), where the preplasma leads to the reflected beam break-up. The dashed ellipses show the images of Ø96 mm calorimeter edge; the images are squeezed due to the oblique observation angle. The energy spectra of accelerated protons at the rear target normal direction are measured with the calibrated time-of-flight or Thomson parabola spectrometer [Fig. 2(e)].

In all experiments, the calorimeters in vacuum were cross-calibrated with the photodiodes or calorimeters which measured leakage through one of the dielectric mirrors. In each shot, the on-target energy was determined from the same leakage. To check the amount of noise, in the experiments B and C we measured the combined contributions of the electrical noise, vibrations, x-rays, and particles with the calorimeter situated at the similar distance from the focus, out of the specular reflection direction. The measured noise (included into the error bars) was at maximum 25 mJ and 40 mJ in the experiments B and C, respectively, but typically of the order of 10 mJ. In addition, in order to estimate the contribution of x-rays and particles to the detected energy in the specular direction, in the experiment B in some shots we put a ~ 1 cm thick uncoated glass lens in front of the calorimeter situated in the specular direction; the reflectivity curve $R(T)$ corrected for the Fresnel reflection was identical to the one obtained without the lens.

The beam cross-section size outside the tight focus was calculated from the geometrical considerations, because in nearly all shots the target shift exceeded the Rayleigh length. The intensity and fluence shown in this paper are the average values over the FWHM spot with the inclusion of the oblique incidence angle effect.

EXPERIMENTAL RESULTS

The dependences of the reflectivity on parameters are shown in Fig. 2. The measured reflectivity curves $R(T)$ [Fig. 2 (a, b)] for both dielectric (polyimide 7.5 and 12.5 μm) and metal (Al 50 nm and 2 μm) targets did not exhibit significant differences. As the intensity near the focus increases, the reflectivity curves dip. The size of the dip depends on the contrast; if the contrast increases the size of the dip (both width and depth) decreases. When the contrast was sufficiently good, the target reflectivity was high even at best focus, where the intensity exceeded 10^{19} W/cm^2. At the lower contrast conditions, the specular reflectivity was high at a distance from the focus (similar to the plasma mirror regime), but dropped to ~ 0 near the focus due to the preplasma formation. The reflectivity decreases in the case of substantially large preplasma due to the reflected beam break-up and an increased absorption [13]. The threshold value of the ASE fluence F_{ASE} where the reflectivity significantly drops, $F_{th} \approx 40$ J/cm^2 [Fig. 2(d)], coincides with the nanosecond laser-induced damage threshold [14], which suggests that the target was disturbed mainly by the ASE rather than possible prepulses. The nearly identical thresholds in the three independent experiments suggest that the absolute error of F_{ASE} was relatively small.

Interestingly, in the highest contrast case, the reflectivity was high, up to 0.75±0.1 in some shots, even in the strongly relativistic regime $a_0 >> 1$, where $a_0 = \left(I_r\left[\mathrm{W/cm^2}\right]\lambda_0^2[\mu\mathrm{m}]/1.37\times10^{18}\right)^{1/2}$ is the dimensionless amplitude; here I_r is the irradiance ($I_r = I/\cos\theta$). This reflectivity is as high as the peak reflectivity achieved by conventional plasma mirrors [8, 10]. We attribute the high reflectivity to lower absorption in the relativistic regime due to the reduced collision rate [15] and absence of the resonance due to the relativistic nonlinearity. The slight fluctuations in specular reflectivity for data taken in experiment A with the plasma mirror [Figs. 2 (b, c)] at $I >$

10^{18} W/cm^2 are attributed to the onset of the preplasma formation, because the estimated ASE fluence of 40 J/cm^2 at best focus coincides with F_{th}.

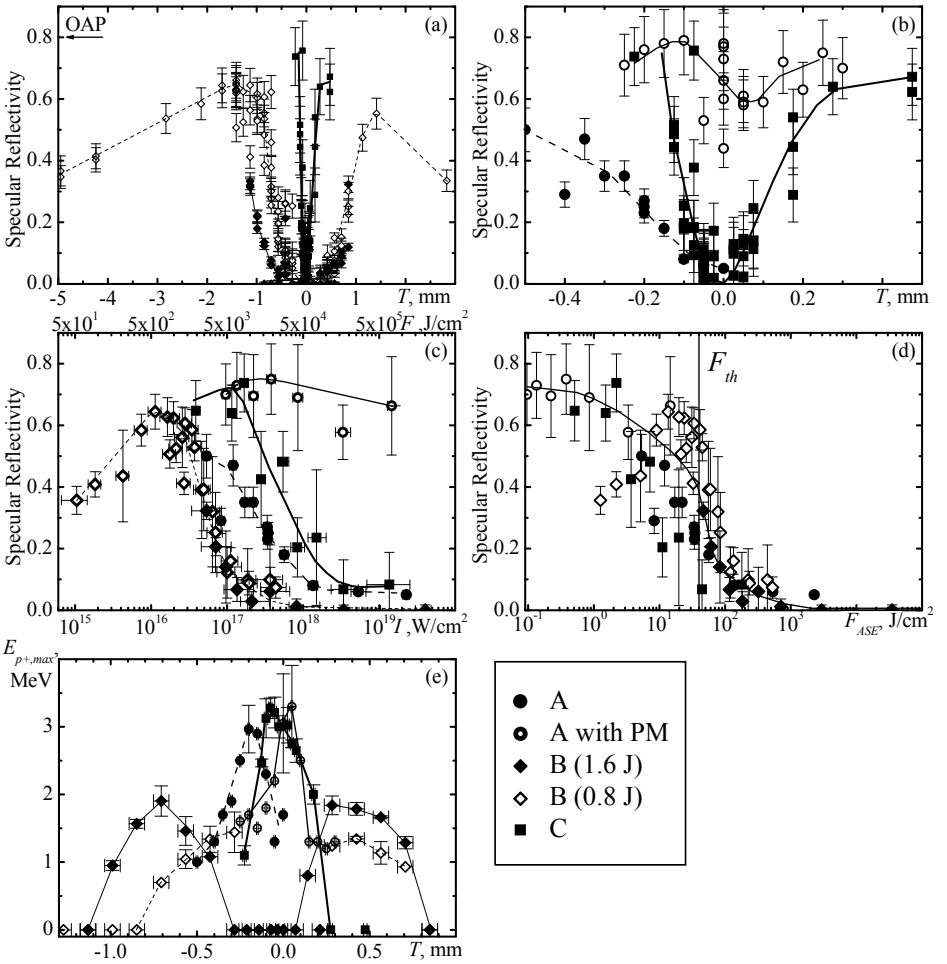

FIGURE 2. The specular reflectivity and maximum proton energy vs. several parameters. The data obtained with three different laser systems (Table 1). The experiment A: the filled and open circles are for the cases without and with the Plasma Mirror (PM). The experiment B: The solid and open diamonds are for the laser energy E_0 = 1.6 J and 0.8 J. The experiment C: the filled squares. (a, b) The specular reflectivity R vs. target position T, note the difference in T range between the frames (a) and (b). (c) The specular reflectivity R vs. the main pulse average intensity I and fluence F; the upper labels are shown for τ_0 = 50 fs. (d) The specular reflectivity R vs. Amplified Spontaneous Emission fluence F_{ASE}. (e) The maximum proton energy in the target normal direction $E_{p+,max}$ vs. target position T. Single-shot data are shown in (a, b), several-shot averages in (c-e). The lines are drawn to guide the eye.

The shape of the reflectivity curve $R(T)$ can be used as a quick and convenient check of the preplasma appearance in the actual shooting conditions. If the preplasma appears, the necessary contrast improvement can be estimated as the ratio of spot area S^* at the target position T^* where the reflectivity starts to drop, to the best focal spot

area S_0. If T^* is outside the Rayleigh length and the laser beam profile can be approximated by a flat-top one, the estimated necessary contrast improvement is

$$K = \frac{S^*}{S_0} = \frac{\pi}{4S_0}\left(\frac{T^*}{f/\#}\right)^2 . \quad (1)$$

In the experiments A and B the detector surface was imaged with a lens onto a CCD. The images of the reflected beam profile revealed the beam break-up at the ASE fluence above ~ 60 J/cm^2. In this case, the laser energy was scattered rather than specularly reflected. With the plasma mirror (experiment A), the beam did not break up even at best focus. This is attributed to plasma formation just before the main pulse peak so that the hydrodynamic motion of the reflecting surface is negligible.

The absolute reflectivity value is not required to judge whether the contrast is sufficient and to estimate the necessary improvement. This allows using a simple screen which is imaged onto a CCD to get a rough dependence $R(T)/R_0$, where R_0 is a calibration constant. To obtain the data similar to those shown in Fig. 2 (a-d), one should sum up the counts inside the original (unperturbed) area of the beam.

The reflectivity measurements presented in this paper were done simultaneously with the proton diagnostic. The single-shot proton energy spectra were measured along the rear target normal direction either with a Thomson parabola ion spectrometer [16] (Experiment A), or time-of-flight spectrometers [17] (Experiments B and C). The dependences of the maximum proton energy vs. the target position are shown in Fig. 2 (e). For both μm and nm thick targets [18], in the high-contrast cases the proton energy was largest at best focus, and gradually decreased when the target was moved to either side. In the low-contrast case, the maximum proton energy decreased near the focus, because the target rear side was disrupted, [19, 20] and far away from focus due to decreasing intensity.

DISCUSSION

The demonstrated technique is convenient and requires relatively simple diagnostics and only tens of laser shots. The technique can be used not only in the ion acceleration experiments, but in other experiments which involve solid target irradiation, too. The absence of large preplasma and therefore high specular reflectivity is the necessary prerequisite for the relativistic harmonics [21] generated by the oscillating mirror [22] or sliding mirror [23] mechanisms. Small preplasmas with scale lengths $<< \lambda/5$ do not prohibit specular reflection of the fundamental and harmonics [24]. We also note that at optimum conditions harmonics can contain a substantial part of the reflected energy [9, 23].

In general, the solid target (preplasma-free) reflectivity remains high when the dimensionless laser amplitude is $a_0 < n_e/n_{cr}$ for thick and $a_0 < \pi n_e l/n_{cr}\lambda_0$ for thin targets [23], respectively [$I_{0,24} < (n_{e,24}\lambda_0)^2$ and $I_{0,24} < (3n_{e,24}l)^2$; here $I_{0,24}$ is the intensity and $n_{e,24}$ is the electron density in the units of 10^{24} W/cm^2 and 10^{24} cm^{-3}, respectively, and λ_0 and the target thickness l are in μm]. For a target moving at relativistic velocity, the corresponding inequalities in the target rest frame should be used. We therefore

believe that the contrast diagnostic based on the specular reflectivity measurement could be validly extended for the intensities up to at least mid-10^{21} W/cm^2 for non-relativistically moving targets. This conclusion is also supported by simulations. For instance, the reflectivity remains high (~ 0.6) at the intensity 5×10^{21} W/cm^2 in 2D PIC simulations for $n_e = 100n_{cr}$, $l \sim 0.4\lambda_0$ to $5\lambda_0$ (the pulse duration is $\tau_0 = 10\lambda_0/c$) [25].

In the described experiments we used relatively short (35-50 fs) pulses. Longer (0.1 to 1 ps) pulses can create a density gradient which results in the increased absorption, or make a hole in the nm-thick target. It would be interesting, therefore, to conduct a separate study of the target reflectivity in this case.

The proposed technique could also be used in the experiments employing the radiation pressure dominant regime of ion acceleration [26] and solid-target relativistic mirror (kagami) [27]. In this case, the frequency downshift and the corresponding reflected energy decrease with time would need to be taken into account.

CONCLUSION

Using three different laser systems we have demonstrated that the specular reflectivity of targets irradiated at full power can be used as the indicator of laser contrast. If the contrast is sufficiently good, the target reflectivity remains high even at ultra-relativistic intensities; in the case of an insufficient contrast, the significant preplasma is formed, and the reflectivity becomes low due to the reflected beam break-up and increased absorption. The technique is relatively simple, robust, works at full laser power, and requires only tens of laser shots. It also allows estimating the necessary contrast improvement in the case of an insufficient contrast. The diagnostic based on the specular reflectivity and/or reflected wavefront characterization can be used to monitor contrast in experiments involving solid target irradiation, in particular, ion acceleration and harmonic generation experiments, including the radiation pressure dominant regime.

ACKNOWLEDGMENTS

This work was supported by the Special Coordination Funds for Promoting Science and Technology (SCF) commissioned by MEXT of Japan, by Korea-China-Japan International Research Collaboration in Development and Applications of Ultrashort High Intensity Laser, by the Ministry of Knowledge and Economy of Korea through the Ultrashort Quantum Beam Facility Program, by the Korea Foundation for International Cooperation of Science and Technology (KICOS) through a grant provided by the Korean Ministry of Education, Science and Technology (MEST) in 2008 (No. K20724000002), and by the U.K. Engineering and Physical Sciences Research Council, Basic Technology scheme “LIBRA” grant No. EP/E035728/1.

REFERENCES

1. G. A. Mourou, T. Tajima, and S. V. Bulanov, *Rev. Mod. Phys.* **78**, 309 (2006).
2. K.-H. Hong, B. Hou, J. A. Nees, E. Power, G. A. Mourou, *Appl. Phys. B* **81**, 447 (2005).

3. N. V. Didenko, A. V. Konyashchenko, A. P. Lutsenko, and S. Y. Tenyakov, *Optics Express* **16**, 3178 (2008).
4. M. Borghesi, A. Giulietti, D. Giulietti, L. Gizzi, A. Macchi, and O. Willi, *Phys. Rev. E* **54**, 6769 (1996); A. Sagisaka, A. S. Pirozhkov, H. Daido, A. Fukumi, Z. Li, K. Ogura, A. Yogo, Y. Oishi, T. Nayuki, and T. Fujii, *Appl. Phys. B* **84**, 415 (2006).
5. E. N. Ragozin A. S. Pirozhkov, A. Yogo, J. Ma, K. Ogura, S. Orimo, A. Sagisaka, M. Mori, Z. Li, and M. Nishiuchi, *Rev. Sci. Instr.* **77**, 123302 (2006).
6. A. S. Pirozhkov, I. W. Choi, J. H. Sung, S. K. Lee, T. J. Yu, T. M. Jeong, I J. Kim, N. Hafz, C. M. Kim, K. H. Pae, Y.-C. Noh, D.-K. Ko, J. Lee, A. Robinson, P. Foster, S. Hawkes, M. Streeter, C. Spindloe, P. McKenna, D. C. Carroll, C.-G. Wahlström, M. Zepf, B. Dromey, K. Markey, S. Kar, Y. T. Li, M. H. Xu, H. Nagatomo, M. Mori, A. Yogo, H. Kiriyama, K. Ogura, A. Sagisaka, S. Orimo, M. Nishiuchi, H. Sugiyama, T. Zh. Esirkepov, H. Okada, S. Kondo, S. Kanazawa, Y. Nakai, A. Akutsu, T. Motomura, M. Tanoue, T. Shimomura, M. Ikegami, I. Daito, M. Kando, T. Kameshima, P. Bolton, S. V. Bulanov, H. Daido, and D. Neely, "Diagnostic of laser contrast using target reflectivity" *Appl. Phys. Lett.* (accepted).
7. P. McKenna, K. Ledingham, I. Spencer, T. McCany, R. Singhal, C. Ziener, P. Foster, E. Divall, C. Hooker, and D. Neely, *Rev. Sci. Instr.* **73**, 4176 (2002).
8. C. Ziener, P. S. Foster, E. J. Divall, C. J. Hooker, M. H. R. Hutchinson, A. J. Langley, and D. Neely, *J. Appl. Phys.* **93**, 768 (2003); B. Dromey, S. Kar, M. Zepf, and P. Foster, *Rev. Sci. Instr.* **75**, 645 (2004).
9. R. Hörlein, B. Dromey, D. Adams, Y. Nomura, S. Kar, K. Markey, P. Foster, D. Neely, F. Krausz, and G. Tsakiris, *New J. Phys.* **10**, 083002 (2008).
10. G. Doumy, F. Quere, O. Gobert, M. Perdrix, P. Martin, P. Audebert, J. Gauthier, J. Geindre, and T. Wittmann, *Phys. Rev. E* **69**, 026402 (2004).
11. J. H. Sung, T. J. Yu, S. K. Lee, T. M. Jeong, I. W. Choi, D.-K. Ko, and J. Lee, *J. Opt. Soc. Korea* **13**, 53 (2009).
12. H. Kiriyama, M. Mori, Y. Nakai, T. Shimomura, M. Tanoue, A. Akutsu, H. Okada, T. Motomura, S. Kondo, S. Kanazawa, A. Sagisaka, J. Ma, I. Daito, H. Kotaki, H. Daido, S. V. Bulanov, T. Kimura, and T. Tajima, *Opt. Comm.* **282**, 625 (2009).
13. P. Gibbon and A. R. Bell, *Phys. Rev. Lett.* **68**, 1535 (1992); M. Borghesi, A. J. Mackinnon, R. Gaillard, O. Willi, D. Riley, *Phys. Rev. E* **60**, 7374 (1999); Y. Ping, R. Shepherd, B. Lasinski, M. Tabak, H. Chen, H. Chung, K. Fournier, S. Hansen, A. Kemp, and D. Liedahl, *Phys. Rev. Lett.* **100**, 085004 (2008).
14. B. Stuart, M. Feit, A. Rubenchik, B. Shore, and M. Perry, *Phys. Rev. Lett.* **74**, 2248 (1995).
15. F. Pegoraro, T. Zh. Esirkepov, and S. V. Bulanov, *Phys. Lett. A* **347**, 133 (2005).
16. D. Neely et al., "Laser ion beam optical spectral control techniques," *AIP Conf. Proc.* (in preparation).
17. S. Nakamura, Y. Iwashita, A. Noda, T. Shirai, H. Tongu, A. Fukumi, M. Kado, A. Yogo, M. Mori, S. Orimo, K. Ogura, A. Sagisaka, M. Nishiuchi, Y. Hayashi, Z. Li, H. Daido, and Y. Wada, *Jpn. J. Appl. Phys.* **45**, L913 (2006); A. Yogo, H. Daido, A. Fukumi, Z. Li, K. Ogura, A. Sagisaka, A. S. Pirozhkov, S. Nakamura, Y. Iwashita, T. Shirai, A. Noda, Y. Oishi, T. Nayuki, T. Fujii, K. Nemoto, I. W. Choi, J. H. Sung, D. K. Ko, J. Lee, M. Kaneda, and A. Itoh, *Phys. Plasmas* **14**, 043104 (2007).
18. D. Neely, P. Foster, A. Robinson, F. Lindau, O. Lundh, A. Persson, C. G. Wahlstrom, and P. McKenna, *Appl. Phys. Lett.* **89**, 021502 (2006); T. Ceccotti, A. Levy, H. Popescu, F. Reau, P. D'Oliveira, P. Monot, J. P. Geindre, E. Lefebvre, and P. Martin, *Phys. Rev. Lett.* **99**, 185002 (2007); P. Antici, J. Fuchs, E. d'Humieres, E. Lefebvre, M. Borghesi, E. Brambrink, C. A. Cecchetti, S. Gaillard, L. Romagnani, Y. Sentoku, T. Toncian, O. Willi, P. Audebert, and H. Pepin, *Phys. Plasmas* **14**, 030701 (2007).
19. A. J. Mackinnon, M. Borghesi, S. Hatchett, M. H. Key, P. K. Patel, H. Campbell, A. Schiavi, R. Snavely, S. C. Wilks, and O. Willi, *Phys. Rev. Lett.* **86**, 1769 (2001).
20. O. Lundh, F. Lindau, A. Persson, C. G. Wahlstrom, P. McKenna, and D. Batani, *Phys. Rev. E* **76**, 026404 (2007); A. Yogo, H. Daido, S. V. Bulanov, K. Nemoto, Y. Oishi, T. Nayuki, T. Fujii, K. Ogura, S. Orimo, A. Sagisaka, J. L. Ma, T. Zh. Esirkepov, M. Mori, M. Nishiuchi, A. S. Pirozhkov, S. Nakamura, A. Noda, H. Nagatomo, T. Kimura, and T. Tajima, *Phys. Rev. E* **77**, 016401 (2008).

21. B. Dromey, M. Zepf, A. Gopal, K. Lancaster, M. Wei, K. Krushelnick, M. Tatarakis, N. Vakakis, S. Moustaizis, and R. Kodama, *Nature Phys.* **2**, 456 (2006); B. Dromey, S. Kar, C. Bellei, D. Carroll, R. Clarke, J. Green, S. Kneip, K. Markey, S. Nagel, and P. Simpson, *Phys. Rev. Lett.* **99**, 085001 (2007).
22. S. V. Bulanov, N. M. Naumova, and F. Pegoraro, *Phys. Plasmas* **1**, 745 (1994).
23. V. A. Vshivkov, N. M. Naumova, F. Pegoraro, and S. V. Bulanov, *Phys. Plasmas* **5**, 2727 (1998). A. S. Pirozhkov, S. V. Bulanov, T. Z. Esirkepov, M. Mori, A. Sagisaka, and H. Daido, Phys. Plasmas **13**, 013107 (2006); *Phys. Lett. A* **349**, 256 (2006).
24. B. Dromey, D. Adams, R. Hörlein, Y. Nomura, S. G. Rykovanov, D. C. Carroll, P. S. Foster, S. Kar, K. Markey, P. McKenna, D. Neely, M. Geissler, G. D. Tsakiris and M. Zepf, *Nature Physics* **5**, 146 2009.
25. T. Zh. Esirkepov, M. Yamagiwa, and T. Tajima, *Phys. Rev. Lett.* **96**, 105001 (2006).
26. T. Zh. Esirkepov, M. Borghesi, S. V. Bulanov, G. Mourou, and T. Tajima, *Phys. Rev. Lett.* **92**, 175003 (2004); A. P. L. Robinson, M. Zepf, S. Kar, R. Evans, and C. Bellei, *New J. Phys.* **10**, 013021 (2008).
27. T. Zh. Esirkepov, S. V. Bulanov, A. G. Zhidkov, A. S. Pirozhkov, and M. Kando, "Laser-driven high-power X- and gamma-ray ultra-short pulse source," *arXiv*:0812.0401 (2008); T. Zh. Esirkepov, S. V. Bulanov, M. Kando, A. S. Pirozhkov, and A. G. Zhidkov, "Boosted high harmonics pulse from a double-sided relativistic mirror," *arXiv*:0902.0860 (2009); *Phys. Rev. Lett.* (accepted).